Application of a multiphase interleaved DC-DC converter for power-to-hydrogen systems

Filippo Pellitteri
Dept. of Engineering
University of Palermo
Palermo, Italy
filippo.pellitteri@unipa.it

Nicola Campagna
Dept. of Engineering
University of Palermo
Palermo, Italy
nicola.campagna@unipa.it

Rosalinda Inguanta
Dept. of Engineering
University of Palermo
Palermo, Italy
rosalinda.inguanta@unipa.it

Rosario Miceli
Dept. of Engineering
University of Palermo
Palermo, Italy
rosario.miceli@unipa.it

***Abstract*—Power electronics plays a crucial role in the implementation of a clean hydrogen production system, whose last stage consists of a water electrolyzer requiring a DC power supply to be in operation. The most recent architectural solutions imply the use of an isolated DC-DC converter, collecting energy from medium voltage (MV) and delivering it to the electrolyzer. An equivalent electrical model of the electrolyzer is therefore needed, as well as an accurate design of the power converter stage, aiming at a high-efficiency operation of the electrolyzer's cells and at a low-ripple supply current, to avoid premature degradation. This work investigates a full-bridge step-down isolated DC-DC converter, focusing on the opportunity of a multiphase interleaved configuration, particularly convenient for the proposed application. The considered maximum power level is 400 kW, representing a small-scale example of an industrial water electrolyzer supplied by a maximum DC voltage of 700 V. Input DC voltage is 7 kV. Power electronics' simulation have been carried out, as well as model analysis of the proposed converter.**

Keywords—DC-DC converters, green hydrogen, water electrolyzer

I. Introduction

In the last few years, hydrogen has been playing an increasingly relevant role in industrial research, due to its notable potential for use in different sectors. Indeed, in addition to conventional applications such as its wide exploitation for ammonia-based fertilizers, pure hydrogen represents an attractive fuel to achieve net zero CO_2 emissions, being able to replace the conventional and polluting fossil fuels, such as carbon and natural gas [1]. This is particularly interesting in relation to the hard-to-abate sectors, i.e. the fossil energy users that are not esasily decarbonisable, such as heavy industry (producers of iron, steel or cement) and heavy transportation (shipping or trucking).

To make hydrogen actually clean, its global production based on steam reforming of natural gas shall be strongly reduced, being this process responsible of CO_2 generation. A more eco-friendly way of producing hydrogen is water electrolysis, a process consisting in the splitting of water into hydrogen and oxygen, while using electrical power. Given that water splitting is not responsible for CO_2 emissions, it is absolutely necessary to guarantee a sustainable production of the electrical energy used in this process to make water electrolysis actually green.

Contribution by renewable energy sources (RES) is therefore essential for this purpose. In recent years, along with the development of alternative RES, incentives have been decided to help the renewable energy sectors [2-7]. At the same time, new power transmission systems, such as high voltage DC (HVDC) lines, have been greatly developed to help RES integration [8-9].

Therefore, even considering the meager amount of hydrogen global production from water electrolysis and the high investments in renewable energy over the last decades, the renewable production of pure hydrogen represents an excellent attempt to achieve net zero carbon emissions by 2050 [10-11].

In such a scenario, hydrogen production and renewable energy sources (RES) perfectly suit each other: while RES contribute to produce clean hydrogen by water electrolysis, hydrogen can represent an energy storage system able to collect the surplus renewable power and possibly give it back during high demands periods thanks to fuel cells, that convert hydrogen into electricity. In this way, it is possibile to compensate the inherently intermittent nature of RES and its negative contribution to the power grid in terms of stability issues [12].

In the general architecture of a clean hydrogen system, shown in Fig. 1, a crucial part of the power-to-hydrogen (P2H) chain is represented by the power conversion required to transfom the electricity arising from RES into the direct current (DC) electricity needed to supply the water electrolyzer. To preserve the electrolyzer, a continuous operation has to privileged, so that a direct connection between photovoltaic/wind energy source shall be possibily avoided without the support of a power grid not to expose the electrolyzer to the fluctuating nature of RES.

Therefore, an integration between RES, power grid and water electrolyzer generally occurs, so that the main P2H block is implemented by the AC-DC power conversion stage between the grid and the electrolyzer.

In this paper, a solution of power system architecture impementing the P2H stage is proposed, with particular focus on the design of an isolated DC-DC converter, notably compliant with the typical costraints of an electrolyzer, such as high DC current, small AC ripple and continuous operation.

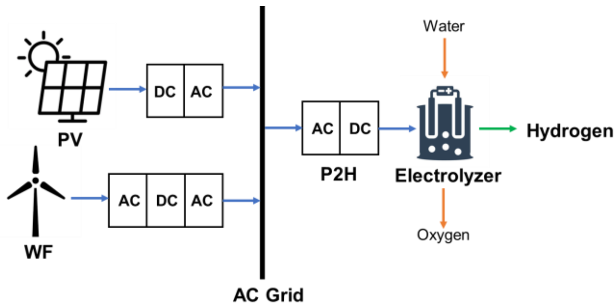

Fig. 1. Power system architecture of a P2H system, with RES integration, based on Photovoltaic plants (PV) and Wind Farms (WF).

II. Hydrogen production: Power system architecture

For large-scale hydrogen production – that is at MW power level - a significant role is played by the P2H power stage, being responsible for the conversion of the medium voltage (MV) electrical power into a DC high-current power flow supplying the electrolyzer, properly controlled in order to modulate the hydrogen production according to the current RES generation [13].

As highlighted by Fig. 1, the P2H stage needs an equivalent electrical model of the hydrogen electrolyzer, which represents the load as seen from the grid side, as well as an accurate design of the actual power conversion system.

A. Electrolyzer electrical model

The electrical parameters of the electrolyzer equivalent model need to be obtained according to a specific electrolyzer, in order to accurately simulate its electrical behaviour. electrical load.

In scientific literature complex models are provided, representing both static and dynamic behaviour [14]. Nevertheless, to emulate the power transfer from source to electrolyzer, a simple resistive model can be used to preliminarly represent the hydrogen electrolyzer as an electric load.

In addition to the electrical model, attention should be paid to the possibility of multi-stack electrolyzers, based either on series or parallel connection.

B. P2H conversion system: typical architectures

The architecture of a P2H conversion system generally implies the connection of a rectifier (AC-DC) stage to the MV AC power grid, featuring a voltage level in the range 6.6-35 kV, through a low frequency transformer (LFT). The typically employed rectifier is the well-known 12-pulse thyristor rectifier, presenting the drawback of requiring bulky additional networks - such as AC filters and reactive compensators – in order to smooth high-order current harmonics and absorb reactive power.

Alternative solutions consist of using an active front end (AFE) rectifier, made of totally controlled switching devices, such as IGBTs, in order to properly shape the input AC current, thus improving high power quality without needing additional networks.

A DC-DC stage can be placed at the rectifer output to enlarge the DC voltage operation range. Nevertheless, a significant inconvenience of such an architecture is represented by the bulky LFTs, so that their elimination is a relevant research challenge. To do that, galvanic isolation shall be implemented between the AC-DC and the elecrolyzer, considering the electrical power chain going from the MV power grid to the hydrogen electrolyzer.

A possible architecture, shown in Fig. 2, implies the use of one AC-DC stage for each of the three phases, converting the MV AC power into the low-voltage DC power directly supplying the electrolyzer. Nevertheless, a more modular approach could be adopted to increase flexibility and reliability.

Therefore, an isolated DC-DC power conversion stage, as shown in Fig. 3, realized through medium or high frequency transformer is needed to reach this goal, thus compacting dimensions. According to the high power level to be transferred and to the possible multi-stack configuration of the supplied electrolyzer, a modular implementation of the DC-DC power conversion stage is a feasible solution.

In this paper, the analysis of a parallel connection between different switching cells of DC-DC stages is investigated, along with the opportunity of a multiphase interleaved configuration, being potentially able to notably smooth the AC ripple in the output DC current, thus bringing benefits to the electrolyzer in terms of reduction of the specific energy consumption and of the degradation level. Indeed, a small AC ripple amplitude would be advantageous to guarantee a long lifespan and to avoid instantaneous null density current values. Furthermore, benefits brought from the increase of the ripple frequency concerning the electrolyzer energy consumption have been demonstrated as well [15-17].

A large electrolyzer is supplied by MW DC power, generally implemented through hudreds Volt and kiloAmpere, so that switching frequencies, even considering the performant emerging technologies of semiconductor devices, shall be in the order of kilo or tenkilo Hertz.

Nevertheless, in order to increase the frequency of the AC part of the electrolyzer supply current, interleaving multiphase approach can be notably convenient.

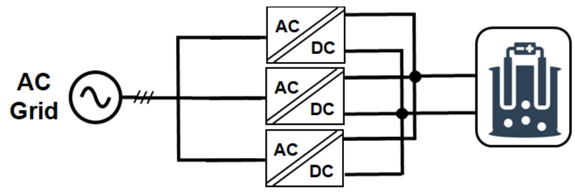

Fig. 2. P2H implementation with one isolated AC-DC stage for each phase.

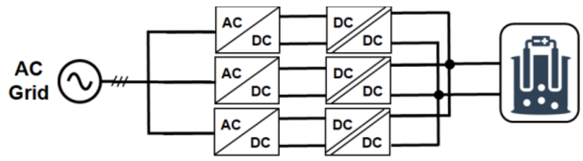

Fig. 3. P2H implementation with AC-DC+DC-DC stages for each phase.

III. DC-DC converter design

The proposed DC-DC stage is implemented through an isolated step-down full-bridge converter, whose schematic is shown in Fig. 4.

A. Analysis and simulations

Active switches of the inverter stage, e.g. M1-M2-M3-M4, are implemented through MOSFETs and modulate power by means of Phase Shift Modulation (PSM).

In Table I the values of the selected parameters are provided, including reactive components and switching devices, as well as the power converters specifications, such as DC voltage, resistive load and target power level.

For the switching devices implementation, power modules of 10 kV SiC MOSFETs have been considered in the inverter stage, whereas power modules of 1200 V SiC Schottky diodes have been considered in the rectifier stage [18-19].

TABLE I. SYSTEM SPECIFICATIONS AND MAIN COMPONENTS

System	*Parameter*	*Description*	*Value*
Converter	V_{in}	Input DC voltage	7 kV
	$V_{out,MAX}$	Maximum output DC voltage	700 V
	$P_{load,MAX}$	Maximum load power	300 kW
	R_{load}	Load resistance	1 Ω
	f_{sw}	Switching frequency	4 kHz
	D	Duty-cycle	0÷0.5
	L	Step-down Inductance	1 mH
MOSFETs	$R_{ds,ON}$	ON Drain-Source Resistance	100 mΩ
	τ_{ON}	Turn-on time	101 ns
	τ_{OFF}	Turn-off time	118 ns
Diodes	V_γ	Conduction forward voltage	1.5 V
Transformer	$N = N_1:N_2$	Turns Ratio	10:1
	L_m	Magnetizing Inductance	10 mH
	L_{lk}	Leakage Inductance	1.5 µH
	R_1	Primary equivalent series resistance	50 mΩ
	R_2	Secondary equivalent series resistance	5 mΩ
Inductance	L	Step-down Inductance	100 µH
Capacitive filters	C_{in}	Input Capacitance	1 mF
	C_{out}	Output Capacitance	100 µF

In Figures 5 and 6 the power electronics simulations are shown, concerning a single stage full-bridge converter, according to the chosen parameters and provided specifications. In the considered example, D is equal to 0.2.

The load voltage V_{out} is related to input voltage V_{in} and input current I_{in} according to the following:

$$V_{out} = \frac{2DV_{in}}{N} - 2V_\gamma - 2R_{ds,ON}I_{in} \tag{1}$$

I_{in} depends on I_{out} according to the transformer turns ratio, as in the folloqing equation:

$$I_{in} = \frac{I_{out}}{N} \tag{2}$$

where I_{out} and V_{out} are:

$$I_{out} = \frac{V_{out}}{R_{load}} \tag{3}$$

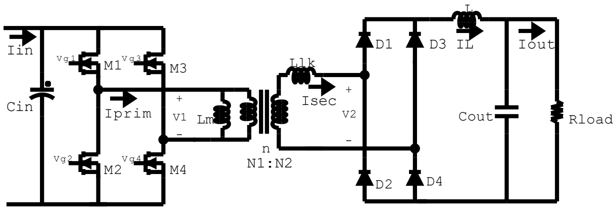

Fig. 4 The proposed isolated DC-DC converter.

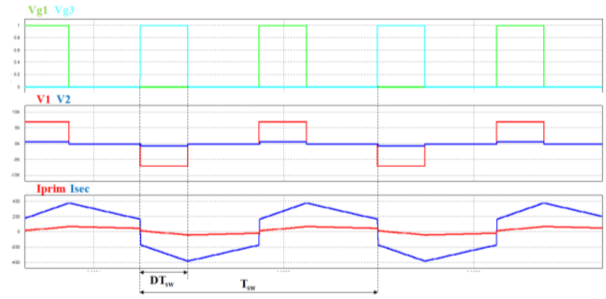

Fig. 5 Simulation of the main waveforms, related to the gate signals with D=0.2.

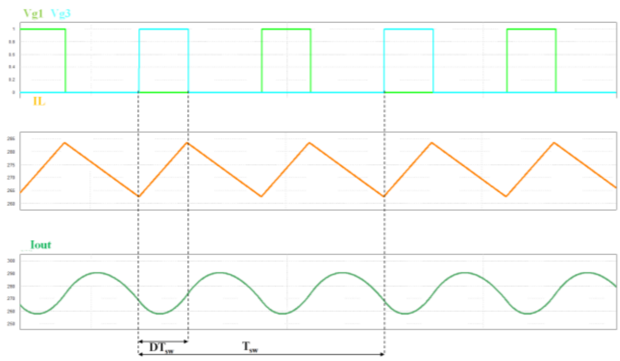

Fig. 6 Simulation of inductance and load current waveforms, related to the gate signals with D=0.2.

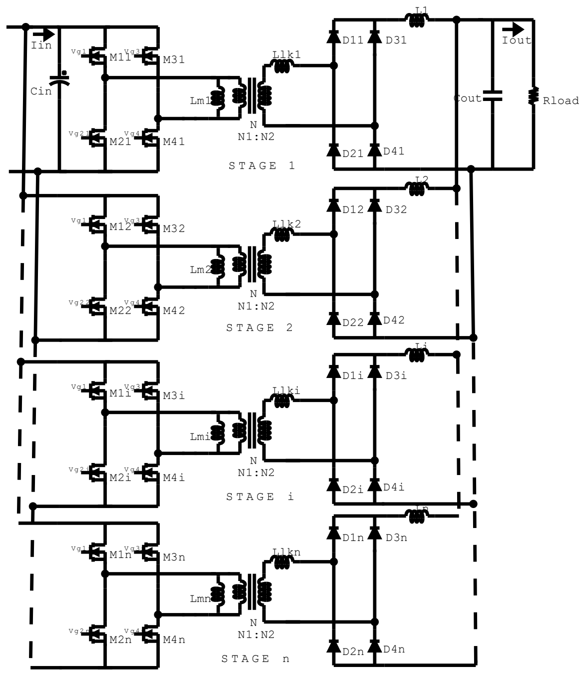

Fig. 7 Interleaved configuration based on n parallel stages.

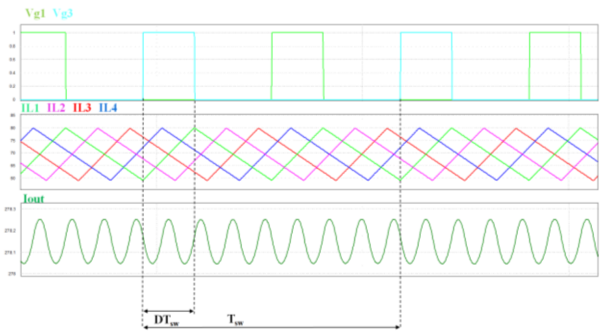

Fig. 8 Simulation of inductance and load current waveforms, related to the gate signals with D=0.2, in a 4-stage interleaved configuration.

According to (1), (2) and (3), and neglecting the forward voltage of diodes, V_{out} arises as the following:

$$V_{out} = V_{in} \frac{2D}{N\left(1+\frac{R_{ds,ON}}{NR_{load}}\right)} \quad (4)$$

A multiphase interleaved paralell configuration has been investigated for the proposed converter, as shown in Fig. 7.

Simulations concerning a 4-stage converter are shown in Fig. 8, highlighting the correct phase difference between the inductance current waveforms. If compared with the 1-stage results, the load current shows a small AC ripple amplitude and a quadruple AC ripple frequency.

B. *Power losses analysis*

Concerning the inverter stage, power losses are divided into conduction losses and switching losses of MOSFETs. AC ripple on current waveforms is neglected so that rms component can be considered equal to DC component. Therefore, conduction losses are:

$$P_{cond,INV} = 2R_{ds,ON} I_{in}^2 \quad (5)$$

During turn-off transients of M1-M2-M3-M4, hard-switching conditions occur, since the load current is still flowing inside the MOSFET while the drain-sourve voltage is rising. During turn-on transients of M1-M2-M3-M4, power losses are only due to conduction of anti-parallel diodes, so that they can be considered null if low forward voltage is present.

$$P_{sw,INV} = E_{sw,INV} f_{sw} \quad (6)$$

$$E_{sw,INV} = 4E_{sw,MOS} \quad (7)$$

$$E_{sw,MOS} = V_{in}(I_{in}/2)(\tau_{ON} + \tau_{OFF}) \quad (8)$$

Concerning the four-diode rectifier, the only power losses are conduction losses, if switching losses are null due to small reverse recovery typical of SiC devices.

$$P_{RECT} = 2V_\gamma I_{out} \quad (9)$$

Transformer copper losses are calculated as in the following:

$$P_{copper,TRANS} = R_1 I_{in}^2 + R_2 I_{out}^2 \quad (10)$$

Therefore, conduction power losses of the i-th inverter stage are:

$$P_{cond,INV,i} = 2R_{ds,ON} \left(\frac{I_{in}}{n}\right)^2 \quad (11)$$

The total conduction power losses related to the n inverter stages are:

$$P_{cond,INV,n} = nP_{cond,INV,i} = 2R_{ds,ON} \frac{I_{in}^2}{n} = \frac{P_{cond,INV}}{n} \quad (12)$$

According to (12), the total conduction losses related to the n inverter stages are n times less than the single-stage configuration.

Switching energy losses of the i-th inverter stage are:

$$E_{sw,INV,i} = \frac{E_{sw,INV}}{n} \quad (13)$$

Therefore, the total switching energy losses related to the n inverter stages are equal to the single stage ones:

$$E_{sw,INV,n} = nE_{sw,INV,i} = E_{sw,INV} \quad (14)$$

The power losses of the i-th rectifier stage are:

$$P_{RECT,i} = 2V_\gamma \frac{I_{out}}{n} \quad (15)$$

Therefore, the total power losses related to the n rectifier stages are equal to the single stage ones:

$$P_{RECT,n} = nP_{RECT,i} = 2V_\gamma I_{out} = P_{RECT} \quad (16)$$

Transfomer copper losses in the i-th stage are calculated as follows:

$$P_{copper,TRANS,i} = R_1 \left(\frac{I_{in}}{n}\right)^2 + R_2 \left(\frac{I_{out}}{n}\right)^2 \quad (17)$$

The total copper losses related to the n transfomer stages are:

$$P_{copper,TRANS,n} = nP_{copper,TRANS,i} = R_1 \frac{I_{in}^2}{n} + R_2 \frac{I_{out}^2}{n} \quad (18)$$

According to (18), the total copper losses related to the n transfomer stages are n times less than the single-stage configuration:

$$P_{copper,TRANS,n} = \frac{P_{copper,TRANS}}{n} \quad (19)$$

C. *Comparison between single- and multi-stage solution*

Therefore, the multiphase interleaved configuration provides benefits in terms of overall power transfer efficiency, since the power losses related to ohmic drops, such as the MOSFETs and copper-related ones, are proportional to the current squared and therefore are reduced by n with respect to the single stage, whereas the switching and diode power losses are proportional to current and consequently are the same as the single stage ones. According to previous equations, an investigation on the power losses for different load power levels has been carried out, highlighting the contributions arising from the different converter sections. Considering D = 0.4 and supposing a fixed 1% contribution to power losses arising from core transformer, Fig. 9 highlights the different contributions as function of the number n of stages.

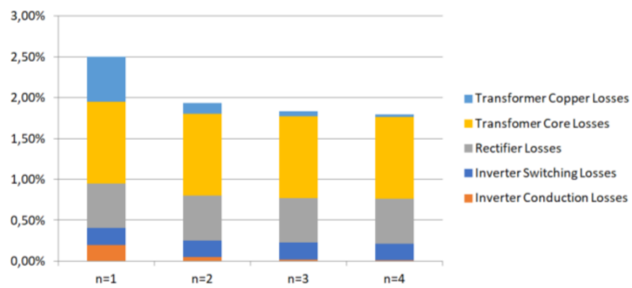

Fig. 9 Different power loss contributions as function of n (D=0.4).

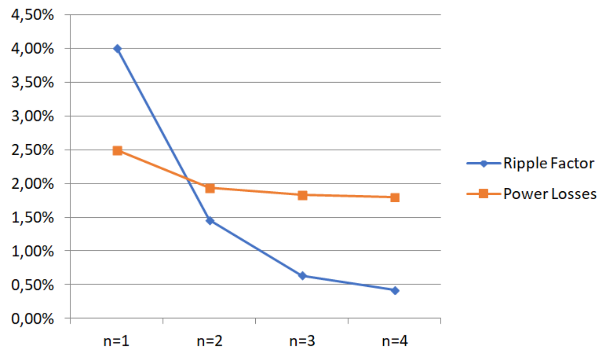

Fig. 10 Overall power losses and load current ripple factor as function of n (D=0.4).

In Fig. 10, overall efficiency and ripple factor as resulting from simulation are plotted as function of the number n of stages, where the ripple factor is defined as the AC ripple amplitude divided by the rms current. Note that the ripple factor evolution decreases, but with a mathematical law dependent on duty-cycle. In the figure example, the considered D is equal to 0.4.

The AC ripple in the load current is notably reduced in the interleaving configuration, as well as the power losses, according to equations. Increase in ripple frequency contributes to increase the electrolyzer cells efficiency, at the cost of a higher degradation, which can be smoothed with a low ripple factor.

IV. Conclusions and Future Developments

In this paper a full-bridge step-down isolated DC-DC converter for hydrogen electrolyzer power supply has been proposed, with maximum power level of 400 kW and a maximum DC voltage of 700 V, with input DC voltage of 7 kV. Power electronics' simulations have been carried out, as well as model analysis of the proposed converter, considering Silicon Carbide (SiC) power modules. The use of a multiphase interleaved parallel configuration has been taken into account as smart solution to smooth AC ripple factor and increase AC ripple frequency of the load current, thus potentially providing benefits to the electrolyzer in terms of durability and efficiency, as well as appropriate to increase power transfer efficiency of the converter. Future developments forecast the experimental implementation of such a solution, with particular research of proper solutions of balanced power sharing between the different interleaved stages and of compact system, in order to maximize power density.

Acknowledgment

This work was realized with the contribution of: PON R&I 2014-2020 (PON R&I FSE-REACT EU), Azione IV.6 "Contratti di ricerca su tematiche Green" to fund and support the research; research project "Sustainable Innovative transport SYtems for MEtropolitan Cities (SISYMEC)", in the frame of the call EUROSTART from University of Palermo, funded by DM 737/2021 of the Italian Ministry of University and Research; SAMOTHRACE - Sicilian Micro and Nano Technologies Research and Innovation Center - SPOKE 3 S2-COMMs (Micro and Nanotechnologies for Smart & Sustainable Communities).

References

[1] Ursua, A.; Gandia, L.M.; Sanchis, P. Hydrogen production from water electrolysis: Current status and future trends. Proc. IEEE 2012, 100, 410–426.

[2] F. Viola, P. Romano, R. Miceli, G. Acciari and C. Spataro, "Piezoelectric model of rainfall energy harvester," 2014 Ninth International Conference on Ecological Vehicles and Renewable Energies (EVER), Monte-Carlo, Monaco, 2014, pp. 1-7, doi: 10.1109/EVER.2014.6844093.

[3] G. Acciari et al., "Piezoelectric Rainfall Energy Harvester Performance by an Advanced Arduino-Based Measuring System," in IEEE Transactions on Industry Applications, vol. 54, no. 1, pp. 458-468, Jan.-Feb. 2018, doi: 10.1109/TIA.2017.2752132.

[4] F. Viola, P. Romano, E. R. Sanseverino, R. Miceli, M. Cardinale and G. Schettino, "An economic study about the installation of PV plants reconfiguration systems in Italy," 2014 International Conference on Renewable Energy Research and Application (ICRERA), Milwaukee, WI, USA, 2014, pp. 989-994, doi: 10.1109/ICRERA.2014.7016534.

[5] F. Pellitteri, P. Livreri, L. Schirone and R. Miceli, "A Hybrid Storage System for Wireless Sensor Nodes powered with Energy Harvesting," 2019 International Conference on Clean Electrical Power (ICCEP), Otranto, Italy, 2019, pp. 221-226, doi: 10.1109/ICCEP.2019.8890178.

[6] V. di Dio, S. Favuzza, D. la Cascia and R. Miceli, "Economical Incentives and Systems of Certification for the Production of Electrical Energy from Renewable Energy Resources," 2007 International Conference on Clean Electrical Power, Capri, Italy, 2007, pp. 277-282, doi: 10.1109/ICCEP.2007.384223.

[7] G. Cipriani, V. Di Dio, N. Madonia, R. Miceli, F. Pellitteri and F. R. Galluzzo, "Reconfiguration strategies to reduce mismatch effects on PV array: An Arduino-based prototype," 2014 International Symposium on Power Electronics, Electrical Drives, Automation and Motion, Ischia, Italy, 2014, pp. 1003-1008, doi: 10.1109/SPEEDAM.2014.6872115.

[8] Imburgia, A.; Romano, P.; Chen, G.; Rizzo, G.; Riva Sanseverino, E.; Viola, F.; Ala, G. The Industrial Applicability of PEA Space Charge Measurements, for Performance Optimization of HVDC Power Cables. *Energies* 2019, *12*, 4186.

[9] P. Romano, R. Candela, A. Imburgia, G. Presti, E. R. Sanseverino and F. Viola, "A new technique for partial discharges measurement under DC periodic stress," *2017 IEEE Conference on Electrical Insulation and Dielectric Phenomenon (CEIDP)*, Fort Worth, TX, USA, 2017, pp. 303-306, doi: 10.1109/CEIDP.2017.8257614.

[10] The "Renewable Molecule": The Potential of Hydrogen from Renewable Energy, White Paper, Orsted. Available online: https: //orsted.com/en/about-us/whitepapers/decarbonising-society-with-power-to-x/power-to-x (accessed on 30 December 2021).

[11] A Hydrogen Strategy for a Climate-Neutral Europe; White Paper; European Commission: Brussels, Belgium, 2020.

[12] Wind Resource: Utilising Hydrogen Buffering–Electrolyser. Available online: http://www.esru.strath.ac.uk/EandE/Web_sites/08-09/Hydrogen_Buffering/Website%20Electrolyser.html (accessed on 11 October 2021).

[13] Chen, M.; Chou, S.-F.; Blaabjerg, F.; Davari, P. Overview of Power Electronic Converter Topologies Enabling Large-Scale Hydrogen Production via Water Electrolysis. *Appl. Sci.* 2022, *12*, 1906. https://doi.org/10.3390/app12041906.

[14] Yodwong, B.; Guilbert, D.; Phattanasak, M.; Kaewmanee, W.; Hinaje, M.; Vitale, G. Proton Exchange Membrane Electrolyzer Modeling for Power Electronics Control: A Short Review. *C* **2020**, *6*, 29. https://doi.org/10.3390/c6020029.

[15] Parache F, Schneider H, Turpin C, Richet N, Debellemanière O, Bru É, Thieu AT, Bertail C, Marot C. Impact of Power Converter Current Ripple on the Degradation of PEM Electrolyzer Performances. Membranes (Basel). 2022 Jan 19;12(2):109. doi: 10.3390/membranes12020109. PMID: 35207031; PMCID: PMC8877858.

[16] Henning P.C. Buitendach, Rupert Gouws, Christiaan A. Martinson, Carel Minnaar, Dmitri Bessarabov, Effect of a ripple current on the efficiency of a PEM electrolyser, Results in Engineering, Volume 10, 2021.

[17] J. Koponen, V. Ruuskanen, A. Kosonen, M. Niemelä and J. Ahola, "Effect of Converter Topology on the Specific Energy Consumption of Alkaline Water Electrolyzers," in *IEEE Transactions on Power*

Electronics, vol. 34, no. 7, pp. 6171-6182, July 2019, doi: 10.1109/TPEL.2018.2876636.

[18] D. Johannesson, M. Nawaz and K. Ilves, "Assessment of 10 kV, 100 A Silicon Carbide mosfet Power Modules," in IEEE Transactions on Power Electronics, vol. 33, no. 6, pp. 5215-5225, June 2018, doi: 10.1109/TPEL.2017.2728723.

[19] "1200V SiC Power Module Dual Diode Pack", Techincal Datasheet. Available online: https://www.rellpower.com/wp/wp-content/uploads/2021/02/GHXS100B120S-D3.pdf